1-1-2020

Experimental evaluation and analytical model of the pressure generated by elastic compression garments on a deformable human limb analogue

Christopher J. Richards
chrisr@uow.edu.au

Julie R. Steele
University of Wollongong, jsteele@uow.edu.au

Geoffrey M. Spinks
University of Wollongong, gspinks@uow.edu.au

Experimental evaluation and analytical model of the pressure generated by elastic compression garments on a deformable human limb analogue

Abstract

© 2020 Compression garments are extensively used for various therapeutic treatments and are expected to deliver accurate and reproducible compression pressures. This study focuses on developing an analytical model to predict the pressure generation by compression garments on human limb analogues. The analogues consisted of non-compressible and compressible cylinders that were chosen as the first step towards evaluating pressure generation on real human limbs. An experimental platform was developed to quantify the relationship between material properties, initial garment extension and pressure. A mathematical model was presented that provided greater accuracy in predicting the pressure generated by compression garments than the existing Young-Laplace equation for compressible limb analogues.

Publication Details

Richards, C., Steele, J. & Spinks, G. (2020). Experimental evaluation and analytical model of the pressure generated by elastic compression garments on a deformable human limb analogue. Medical Engineering and Physics,

Experimental Evaluation and Analytical Model of the Pressure Generated by Elastic Compression Garments on a Deformable Human Limb Analogue

Christopher J. Richards[1], Julie R. Steele[2], Geoffrey M. Spinks[1]

[1]Intelligent Polymer Research Institute, University of Wollongong, Wollongong, Australia

[2]Biomechanics Research Laboratory, University of Wollongong, Wollongong, Australia

---

Abstract

Compression garments are extensively used for various therapeutic treatments and are expected to deliver accurate and reproducible compression pressures. This study focuses on developing an analytical model to predict the pressure generation by compression garments on human limb analogues. The analogues consisted of non-compressible and compressible cylinders that were chosen as the first step towards evaluating pressure generation on real human limbs. An experimental platform was developed to quantify the relationship between material properties, initial garment extension and pressure. A mathematical model was presented that provided greater accuracy in predicting the pressure generated by compression garments than the existing Young-Laplace equation for compressible limb analogues.

Keywords: pressure, compression, analytical, model, prediction

---

Corresponding author:
Senior Professor Geoffrey M. Spinks
Intelligent Polymer Research Institute
University of Wollongong
Northfields Avenue
Wollongong, New South Wales, 2522, AUSTRALIA
Email: gspinks@uow.edu.au

April 2020

1. Introduction

Compression garments are designed to apply external pressure to the wearer through the use of close-fitting stretch fabrics. These garments are extensively used for a variety of applications such as aesthetic body-shaping, improving recovery after exercise, and as medical therapy for various conditions. In medical use compression garments are usually designed to prevent excessive swelling. Vessels that carry fluid in human tissue, such as lymphatic vessels, can be deformed under the garment pressure, creating a pressure gradient between the compressed region and the non-compressed region of a limb or the body. The pressure gradient applied by the garment restricts fluid from flowing into the compressed area and/or pushes out the fluid residing within the affected body area. Compression garments can therefore either prevent or reduce swelling and can assist in reducing the discomfort of injuries and certain diseases [1].

To be used for medical therapies and treatments, compression garments need to deliver reproducible and accurate pressures. The desired pressure is defined by various national standards governing medical compression devices, such as compression stockings. For example, in Germany, France and Australia the 'compression-class' of a compression device is defined by the magnitude of pressure applied by a garment to the circumference of a non-compressible ankle analogue and the RAL-GZ 387/1 standard has been frequently used to assess compression garments [2, 3]. In previous research [4] the standards for compression garments have been evaluated experimentally using garments applied to non-compressible limb analogues. Several studies have shown that the Young-Laplace relation describes how the elastic strain in a garment stretched over a non-compressible cylinder relates to the pressure experienced at the garment-cylinder interface [4-10] as described by Equation 1 [7, 8, 10-15]:

$$P = \frac{T}{r} \qquad \text{(Eq. 1)}$$

where P is the interfacial pressure experienced by a cylinder of radius r; and T is the tension in the compression garment per unit width of the garment. Elastic stretching of the compression garment introduces the wall tension and the pressure applied to the limb. The tension for a compression garment is then calculated by Equation 2, assuming Hookean properties of the garment:

$$T_G = \frac{k(2\pi r_G - l_0)}{w_G} \quad \text{(Eq. 2)}$$

Here k is the strain-independent stiffness of the garment, l_o is the initial length of the garment and w_G and r_G are the final width and radius of the garment, respectively. The simplest application to non-compressible limbs assumes that $r_G' = r_G = r$ and $w_G' = w_G$. These conditions will not hold true for compressible limbs with $r_G' < r_G$ leading to a loss of tension in the garment and reduced pressure generation. Not surprisingly, studies examining compression garment behaviour on human limbs have shown significant differences between the expected pressure from theoretical calculations (Equation 1) and the actual measured pressure [10, 16]. Compared to its uncompressed state, a real human limb can be compressed to a smaller radius, which reduces tension in the garment (Equation 2) and, in turn, generates lower than expected pressures. The amount real limbs can be compressed, however, varies from person to person due to individual variability in human tissue properties [17, 18]. It is therefore difficult to specify the actual pressure that will be generated between a compression garment and a human limb.

Current theories lack the key factors that accurately describe the deformation associated with compressible geometries under loading from compression garments. This issue is further complicated when the highly variable geometry and complex structure of a human limb is considered. The complexities outlined above create a problem when trying to design a compression garment on a deformable human limb to match a specific pressure range. A theoretical model that accurately describes the geometric, mechanical and material properties

of both the garment and a human limb is therefore necessary to design effective compression garments, which can generate specific pressures in desired ranges for medical applications. As a first step towards this objective, the present study aimed to experimentally investigate the pressure generated by compression garments applied to both compressible and non-compressible limb analogues. An analytical approach was developed that encompassed the mechanics of the experimental findings, to estimate the pressure, and was compared to the pressure predicted from Equation 1.

2. Experimental methods

Two types of limb analogues were fabricated to represent a compressible limb and a non-compressible limb (see Figure 1). Both of these limb analogues were regular and cylindrical in geometry, with the same diameter. The compressive modulus of the compressible limb analogue was chosen because it was within the regime of human soft tissues between 5 kPa to 140 MPa [19]. These simple systems were chosen so that the pressure predicted by the Young-Laplace equation could be accurately calculated and compared to the experimentally-measured pressure. The pressure was measured using calibrated capacitive-based pressure sensors (active sensor area: 0.785 cm^2; sensor model number S2011-PEX518; Pliance® Novel, Germany). This pressure measurement system was used due to its low profile (approximately 2 mm thick) and flexible nature, so that bending of the sensor to match the curvature of the cylinder surface had negligible effect on the pressure measurements.

2.1. Compression garments

Exercise band material (66fit, Lincolnshire, UK) was used to fabricate custom closed-loop compression garments. The exercise bands came in continuous lengths in a variety of thicknesses, which were used to represent compression garments of varying stiffness. Uniaxial tensile testing of the material (Shimadzu EZ-L testing machine, Shimadzu, Japan) allowed the modulus and stiffness to be calculated and used in theoretical calculations of pressure

generation. The compression garments were fabricated from a range of thicknesses (0.36 mm, 0.30 mm, 0.26 mm and 0.20 mm) and a range of diameters (90%, 80%, 70% and 60% of the initial circumference of the limb analogue), resulting in 16 total configurations tested in triplicate. All garments were 130 mm wide. A new garment was fabricated for each measurement.

2.2 Non-compressible limb analogue

Plastic polyvinyl chloride (PVC) pipe of 80 mm diameter was cut to a length of 300 mm. The wall thickness of the pipe was 4.0 ± 0.25 mm (Figure 1). The thickest and shortest compression garment was placed onto the pipe because this represented the maximum loading limits that occurred during pressure measurement testing. The diameters of the pipe across a range of radial and height locations showed negligible difference between the compressed and non-compressed regions so the pipe could be considered incompressible over the pressure ranges used in the present study. The pressure sensor was adhered directly onto the surface of the pipe (using the sensor mounting tabs) and the resultant garment-surface interface pressure was measured immediately about the midline of the garment's width using the Pliance® Novel software. Pressure measurements were repeated for all 16 compression garment thicknesses and diameters.

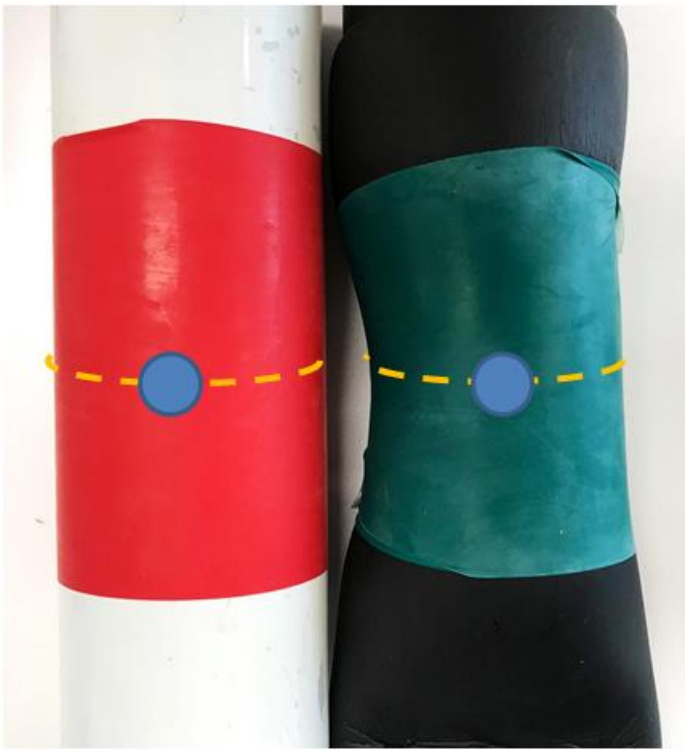

Figure 1. The non-compressible (left) and compressible (right) limb analogues. The pressure sensor was located underneath the compression garment, at about the middle of the width (dotted line) of the compression garment, as indicated by the solid dot.

2.3 Compressible limb analogue

High density polyurethane foam was used as a surrogate for a compressible limb analogue. The foam was formed into a cylinder shape to match the dimensions of the non-compressible limb analogue (80 mm diameter and 300 mm in length). The mechanical properties of the compressible foam were measured (Shimadzu EZ-L testing machine, Shimadzu, Japan) on a cube shape using uniaxial compression testing. A pressure sensor was placed at the midpoint of the cylinder's length and the resultant pressure was recorded for the range of compression garments using the same methods described for the non-compressible limb analogue. The deformation of the cylinder was recorded using a non-elastic string about the smallest circumference (at the midpoint of the cylinder's length) at zero tension. The radial deformation was calculated from the measured circumference.

3. Analytical derivation of interface pressure

The analytical process described below was adapted from the analysis of tubular press fittings [19] and is used here to estimate the limb compression, based on the following assumptions:

(i) friction between the surfaces was negligible,

(ii) materials are Hookean in behaviour,

(iii) the geometry was maintained uniform and regular, and

(iv) radial compression of the cylinder behaved in the same manner as uniaxial compression.

For a given compression garment of initial radius r_G placed onto a cylinder geometry of initial radius r_C, the garment must have a smaller radius than the cylinder ($r_G < r_C$) to generate pressure at the garment-cylinder interface. The pressure at the interface will cause radial deformation of the cylinder geometry (u_C) proportional to the stresses and material characteristics to a new radius R given by [20]:

$$u_C = \frac{r_C}{E_C}(\sigma_{\theta C} - v_C\sigma_{rC}) \quad \text{(Eq. 3)}$$

where E_c is the Young's Modulus of the cylinder, $\sigma_{\theta C}$ is the hoop stress at the interface, σ_{rC} is the radial stress at the interface and v_C is the Poisson's ratio of the cylinder. Likewise, as the cylinder is compressed, the compression garment undergoes radial deformation of u_G[20]:

$$u_G = \frac{r_G}{E_G}(\sigma_{\theta G} - v_G\sigma_{rG}) \quad \text{(Eq. 4)}$$

where E_G is the Young's Modulus of the garment, $\sigma_{\theta G}$ is the hoop stress at the interface, σ_{rG} is the radial stress at the interface and v_G is the Poisson's ratio of the garment. A graphical representation of these terms is shown in Figure 2 for the garment and cylinder before and after compression has occurred.

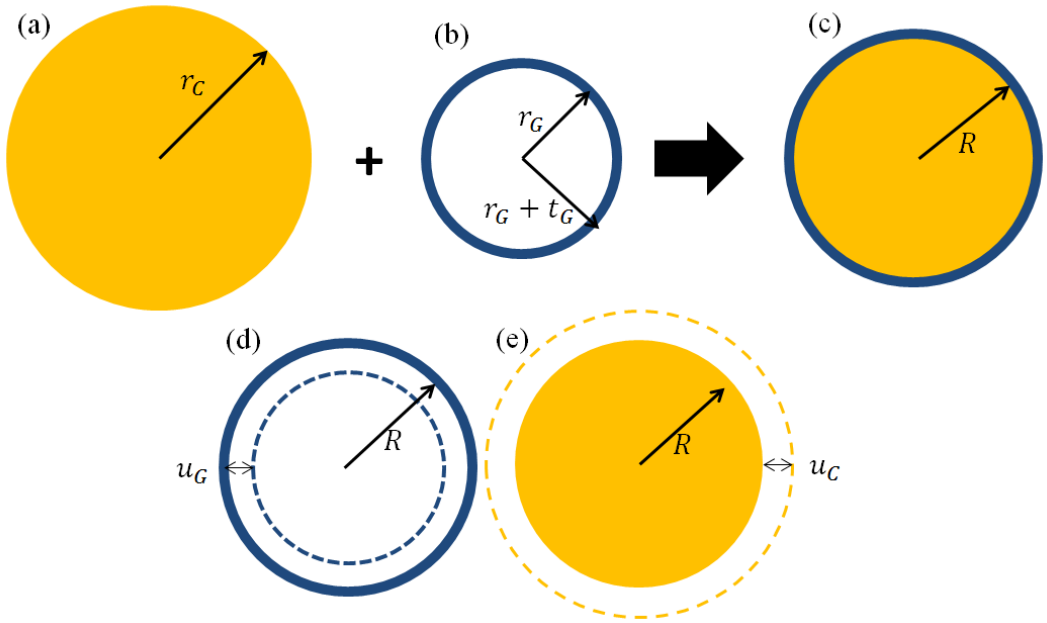

Figure 2. Graphical representation of the geometrical components of the analytical model. The initial interfacing radii of the cylinder (a) and compression garment (b) are given by $\boldsymbol{r_C}$ and $\boldsymbol{r_G}$, respectively. The thickness of the garment is $\boldsymbol{t_G}$. The garment causes compression of the cylinder (c) to a new interfacial radius of $\boldsymbol{R}$, resulting in radial deflections of $\boldsymbol{u_G}$ and $\boldsymbol{u_C}$ for the garment (d) and cylinder (e), respectively.

The general form for determining hoop stress for a thick-walled cylinder under pressure (p) with an inner radius of r_i and outer radius of r_o is given by [20]:

$$\sigma_\theta = -p\frac{r_o^2+r_i^2}{r_o^2-r_i^2} \quad \text{(Eq. 5)}$$

For a compression garment the inner radius becomes the initial inner radius of the garment ($r_i = r_G$) and the outer radius is the inner radius in addition to the garment thickness ($r_o = r_G + t_G$). Therefore, modifying Equation 5 for the garment's hoop stress ($\sigma_{\theta G}$) at the interface takes the form of:

$$\sigma_{\theta G} = -p\frac{(r_G+t_G)^2+r_G^2}{(r_G+t_G)^2-r_G^2} \quad \text{(Eq. 6)}$$

Similarly, for a solid cylinder (i.e. $r_i = 0$ for the cylinder used in this study) calculating the cylinder's hoop stress ($\sigma_{\theta C}$) can be simplified to:

$$\sigma_{\theta C} = -p \quad \text{(Eq. 7)}$$

The radial stress is simply the negative of the garment-cylinder interface pressure:

$$\sigma_{rC} = \sigma_{rG} = -p \quad \text{(Eq. 8)}$$

Substituting these measurable parameters into the deflection equations yields a cylinder deformation of:

$$u_C = -\frac{r_C}{E_C} p(1 - v_C) \quad \text{(Eq. 9)}$$

and for the compression garment deformation:

$$u_G = \frac{r_G}{E_G} p \left[\frac{(r_G + t_G)^2 + r_G^2}{(r_G + t_G)^2 - r_G^2} + v_G \right] \quad \text{(Eq. 10)}$$

As the final radial deformation of both the garment and the cylinder is between the initial garment and cylinder radii, the constraint is given:

$$u_G - u_C = r_C - r_G \quad \text{(Eq. 11)}$$

Substitution of u_C (Equation 9) and u_G (Equation 10) into Equation 11 and solving for pressure (p) gives:

$$p = \frac{r_C - r_G}{\frac{r_G}{E_G}\left[\frac{(r_G + t_G)^2 + r_G^2}{(r_G + t_G)^2 - r_G^2} + v_G\right] - \frac{r_C}{E_C}(1 - v_C)} \quad \text{(Eq. 12)}$$

Equation 12 allows the pressure values to be calculated using initial parameters of the compression garment-cylinder system. Poisson's ratio for the elastic garments was assumed as 0.5 (a typical value for rubber-like materials) and as 0 for the foam cylinder [21, 22]. Calculated pressure values from Equation 1 and Equation 12 were compared for concordance to the experimentally measured values for the compressible and non-compressible limb analogues using Lin's Concordance Correlation Coefficients (Microsoft Excel 2010). This allowed the level of agreement of values predicted by the Young-Laplace equation and the proposed analytical equation to be determined relative to the experimental data, using shared expected values between each case. The level of agreement characterised by each Lin's coefficient (*Lin's* r_c) was deemed poor (r_c<0.50), low (0.50<r_c<0.70), moderate (0.70<r_c<0.80), high (0.80<r_c<0.90) and excellent (r_c>0.90) [23]. The final radius at the

garment-surface interface was also calculated by substituting the calculated pressure value from Equation 12 into Equation 9, allowing the resultant radii to be calculated for each experiment.

4. Experimental results

Uniaxial tensile testing of the 16 closed-loop compression garments resulted in an average Young's Modulus of 2.0 ± 0.6 MPa for all garments. The modulus was calculated within the domain of strain experienced by the compression garments during the pressure measurements. Uniaxial compression testing of the foam used to construct the compressible limb analogue resulted in an average modulus of 47.6 ± 0.9 kPa. The compressive modulus was measured along the radial direction in the cylinder geometry.

The pressure measured at the garment-surface interface for the non-compressible and compressible limb analogues is shown in Figure 3 and Figure 4, respectively, for each thickness of compression garment. Pressure values are reported according to the size of the compression garment relative to the starting cylinder diameter (as opposed to the final diameter of the compressible cylinder). The pressure estimated by the Young-Laplace equation exhibited excellent agreement to the experimentally measured pressure on the non-compressible cylinder (*Lin's* $r_c = 0.97$). However, for a given garment thickness and initial garment length, the pressure generated on the compressible analogue was consistently less than that generated on the non-compressible cylinder. Comparing the Young-Laplace and experimentally measured compressible cylinder values revealed low agreement (*Lin's* $r_c = 0.69$). Values produced by the model described in this study showed greater agreement with the experimentally measured pressure values (*Lin's* $r_c = 0.74$), although higher pressure configurations exhibited deviations. When these deviations (bands sized at 60% the cylinder radius at 0.36 mm thickness) were excluded the agreement increased greatly (*Lin's* $r_c = 0.87$), suggesting the model does not hold for higher tension and deformation conditions. A comparison of the calculated and

experimentally measured radii has been plotted in Figure 5. Again, the plots are with respect to the initial size of the compression garment relative to the starting cylinder diameter. Differences between the expected and experimentally measured diameters resulted in poor agreement (*Lin's* r_c = 0.20).

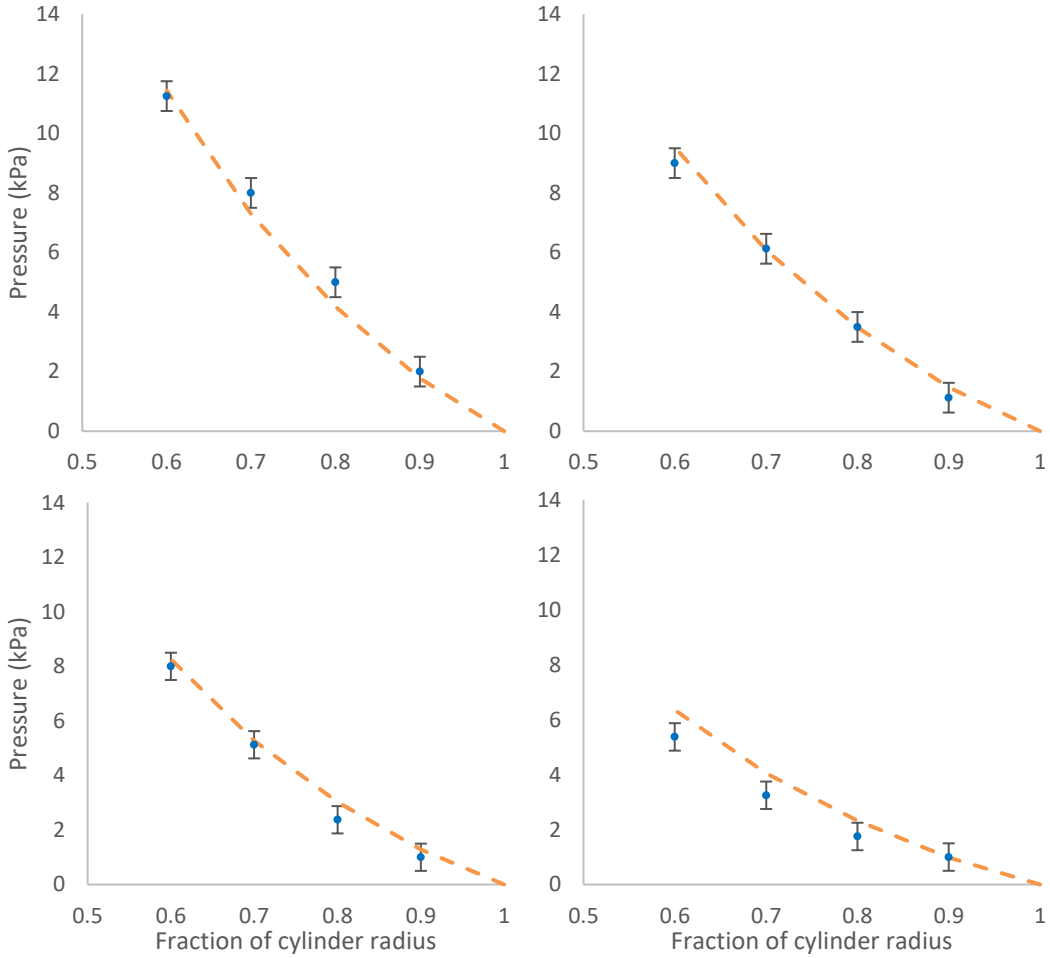

Figure 3. Plots of the experimentally-measured pressure values for the non-compressible limb analogue (circles) versus the pressure value calculated using the Young-Laplace equation (dashed line). Each plot represents one thickness of compression garment over a range of sizes. The thicknesses are, from top left, 0.36 mm, 0.30 mm, 0.26 mm, 0.20 mm.

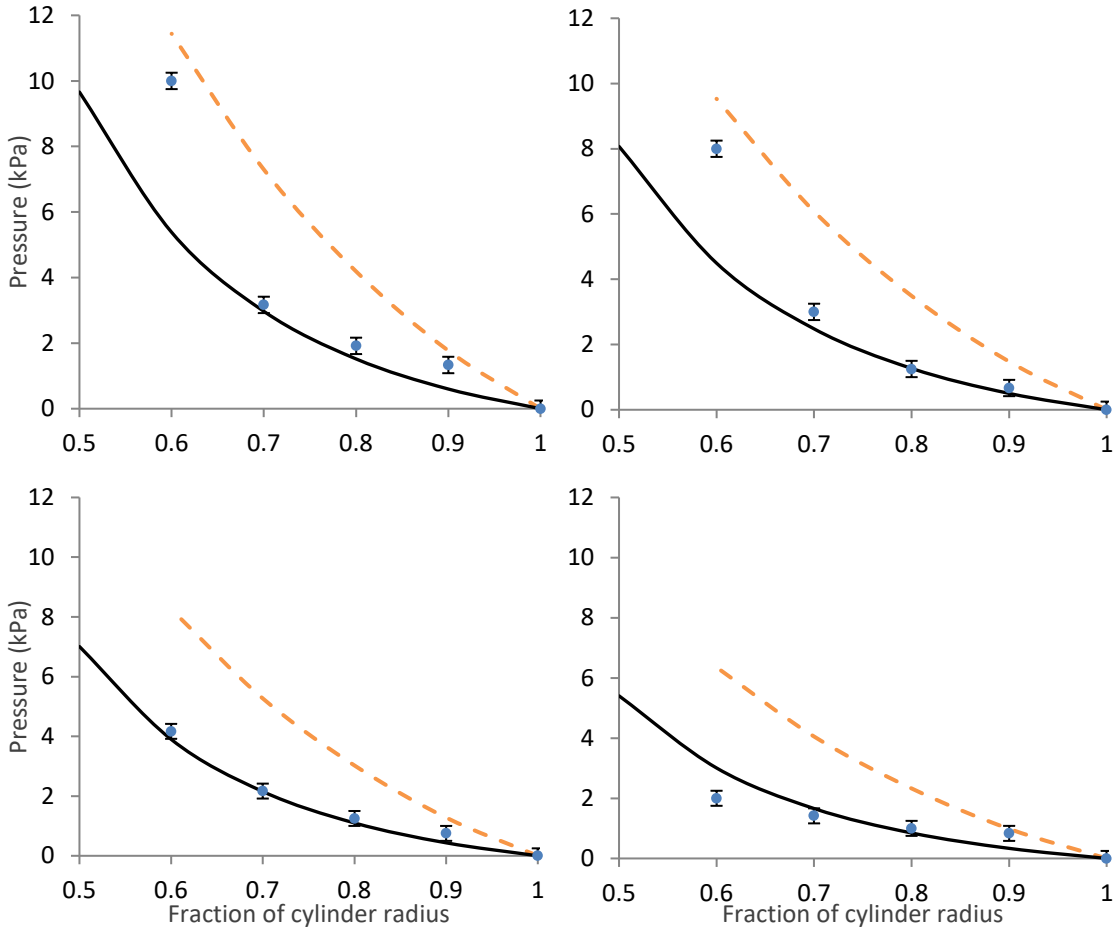

Figure 4. Plots of the experimentally-measured pressure values (circles) for the compressible limb analogue versus the pressure values calculated by the derived analytical model (solid line) and the Young-Laplace equation (dashed line). Each plot represents one thickness of compression garment over a range of sizes. The thicknesses are, from top, left 0.36 mm, 0.30 mm, 0.26 mm, 0.20 mm.

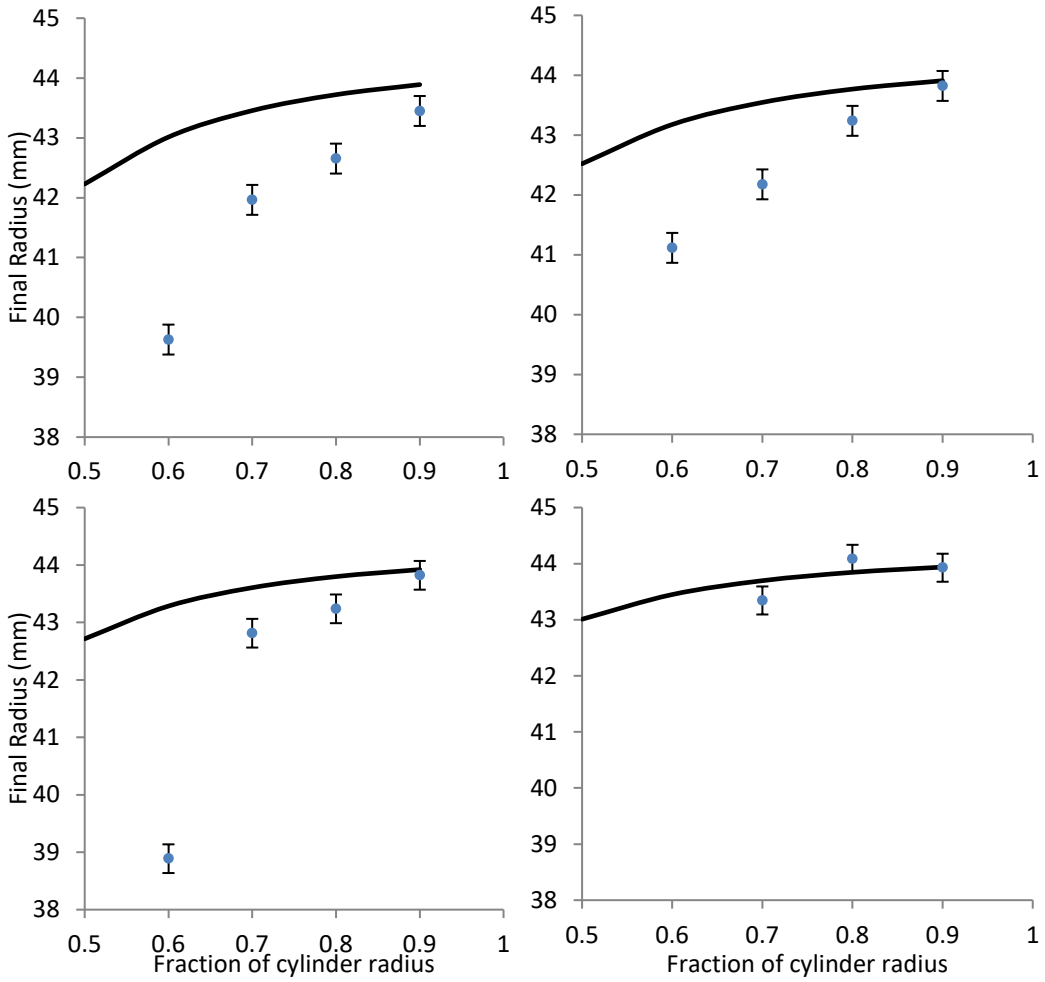

Figure 5. Plots of the experimentally-measured final radii (circles) for the compressible limb analogue versus values calculated by the derived analytical model (solid line). Each plot represents one thickness of compression garment over a range of sizes. The thicknesses are, from top left, 0.36 mm, 0.30 mm, 0.26 mm, 0.20 mm.

6. Discussion

The good agreement between the pressure values predicted by the Young-Laplace equation to the experimentally-measured pressure values on the non-compressible limb analogue was consistent with previous research [7, 8, 10-15] and thereby validates the experimental setup. In contrast, however, only low agreement was found between the experimentally-measured pressure values for the compressible limb analogue and the predicted Young-Laplace pressure values, whereby the predicted pressure values overestimated the actual measured pressure.

As shown in Figure 4, the pressure values predicted using the new model were similar to the experimental values in most cases with a significant improvement compared with the Young-Laplace equation. The predicted values, however, were lower than the experimentally-measured values in cases where the compression garment exhibited high tension. This discrepancy was observed for garments 0.36 mm and 0.30 mm thickness with an initial length at 60% of the cylinder's initial circumference. It was observed in these cases that the foam cylinder deformation was large and non-uniform with respect to the change in radius across the width of the garment, as shown in Figure 1. The obvious non-uniform strain distribution invalidates the assumption that the cylinder would maintain regular and uniform geometry. However, the other predicted pressure values exhibited high agreement with the experimentally-measured pressure values and the non-uniform deformation was less obvious.

Calculations of the final radii were consistently larger than the measured values with the discrepancy greatest when the garment generated the highest pressures. Again, it is likely that the non-uniform deformation of the cylinder across the band width contributed to the error in the calculated radii. The reported measured radii were taken at the mid-point of the compression garment where the radii were smallest. As seen in Figure 1, the variation in radius across the band width could be several millimetres in magnitude, which is sufficient to account for the discrepancies between the measured and calculated radii.

Existing models used to describe pressure also do not account for non-linear mechanical properties typical of elastomeric materials [24]. Apparent non-linear effects are also likely to arise from the complex internal stresses experienced inside the cylinder geometry [25]. Computational numerical approaches, such as Finite Element Analysis (FEA), would allow the compression garment-limb system to be modelled to the required level of detail, potentially accounting for complexity of human limbs and including the non-linear material properties of the elastic garment. FEA, however, usually requires an initial loading condition, which is then

applied to the geometry (the system is simplified to a mesh structure), that causes strain, and therefore stress, in the geometry. In this particular case, the compression garment would generate the initial loading conditions over the geometry it is placed upon, which is an interesting challenge to calculate in itself. The loading provided by the garment is also not constant, as shown in the derivation of the analytical model, because as deformation occurs the tension in the garment changes proportionally to the tensile properties of the material. Further extension of the model presented here would be applicable to such kinds of computational simulations of pressure generation. Experimental validation of computational models would also be required using a benchtop system, such as the compressible limb analogue described above. A validated computational model would be useful as a tool for designing customised compression garments that generate specific pressures and thereby the desired physiological effects.

By understanding the relationship between the stiffness of a garment and the human body, clinicians and therapists would have a better understanding of the resultant interfacial pressure. The correct size, form and stiffness of compression garments could be driven by the individual characteristics of the patient. Furthermore, practical measurements of limb circumference using non-elastic measuring tapes, for compression garment sizing, generates tension within the measuring tape leading to pressure on the limb and, in turn, causing deformation and a lower than actual limb circumference being recorded. Consequently, a garment based on these measurements will be tailored for limbs of smaller size and would likely deliver a higher than expected pressure. The review and assessment of the veracity of clinical practices may benefit from these understandings.

7. Conclusions

The success of medical-based compression therapies relies on delivering the correct amount of pressure to the human body and this study has highlighted the difficultly in estimating the exact

pressure caused by a compression garment due to the underlying mechanics. Understanding how pressure is developed on a uniform, synthetic compressible limb analogue provides an insight into these mechanics and has been demonstrated in this study. The Young-Laplace equation did not account for compressibility of the limb analogue. Therefore, an analytical model was adapted to encompass the response of the compressible material to the pressure applied by the compression garment. Pressure values provided by this model showed excellent agreement with experimentally-measured values, except at the largest deformations. Future extensions of the model using computational approaches are proposed in an effort to include the non-linear and non-uniform behaviours of the system. It is recommended that the additional information provided by such an approach would allow pressure values to be predicted with greater accuracy. This effort would ultimately lead to a validated computational model as a method to design effective compression garments, which accurately deliver the desired pressures.

8. Declaration of interest

All authors have no competing interests to disclose.

9. References

1. Moseley, A.L., Carati, C.J., and Piller, N.B., *A systematic review of common conservative therapies for arm lymphoedema secondary to breast cancer treatment.* Annals Of Oncology: Official Journal Of The European Society For Medical Oncology, 2007. **18**(4): p. 639-646.
2. BSI, *Specification for graduated compression hosiery*. 1985, BSI: BSI
3. Deutsches institut für gütesicherung und kennzeichnung , E.V., *Medical Compression Hosiery*, in *Quality Assurance RAL-GZ 387/1*. 2008, RAL Deutsches Institut für Gütesicherung und Kennzeichnung e.V.
4. Ghosh, S., Mukhopadhyay, A., Sikka, M., and Nagla, K.S., *Pressure mapping and performance of the compression bandage/garment for venous leg ulcer treatment.* Journal Of Tissue Viability, 2008. **17**(3): p. 82-94.
5. Bhattacharya, S., Shaikh, T., and Purushottam Solao, R., *Development of prototype bandage lapper for constant tension bandaging required for effective medical-clinical treatments.* J Tissue Viability, 2012. **21**(2): p. 54-63.
6. Lisa, M., Margot, B., and Phil, W., *The study of pressure delivery for hypertrophic scar treatment.* International Journal of Clothing Science & Technology, 2004. **16**(1/2): p. 173-183.
7. Macintyre, L., *Designing pressure garments capable of exerting specific pressures on limbs.* Burns, 2007. **33**: p. 579-586.
8. Thomas, S., *The production and measurement of sub-bandage pressure: Laplace's Law revisited.* Journal Of Wound Care, 2014. **23**(5): p. 234.
9. Yamada, T. and Matsuo, M., *Clothing Pressure of Knitted Fabrics Estimated in Relation to Tensile Load Under Extension and Recovery Processes by Simultaneous Measurements.* Textile Research Journal, 2009. **79**(11): p. 1021-1033.
10. Yıldız, N., *A novel technique to determine pressure in pressure garments for hypertrophic burn scars and comfort properties.* Burns, 2007. **33**: p. 59-64.
11. Khaburi, J.A., Nelson, E.A., Hutchinson, J., and Dehghani-Sanij, A.A., *Impact of multilayered compression bandages on sub-bandage interface pressure: a model.* Phlebology, 2011. **26**(2): p. 75-83.
12. Al Khaburi, J., Dehghani-Sanij, A.A., Nelson, E.A., and Hutchinson, J., *Effect of bandage thickness on interface pressure applied by compression bandages.* Medical Engineering and Physics, 2012. **34**: p. 378-385.
13. Sikka, M.P., Ghosh, S., and Mukhopadhyay, A., *Mathematical modeling to predict the sub-bandage pressure on a conical limb for multi-layer bandaging.* Medical Engineering & Physics, 2016. **38**(9): p. 917-921.
14. Lee, G., Rajendran, S., and Anand, S., *New single-layer compression bandage system for chronic venous leg ulcers.* British Journal of Nursing, 2009. **18**(15): p. S4-18.
15. Todd, M., *Compression bandaging: types and skills used in practical application.* British Journal of Nursing, 2011. **20**(11): p. 681-687.
16. Hill, J., Howatson, G., Someren, K., Davidson, S., and Pedlar, C., *The variation in pressures exerted by commercially available compression garments.* Sports Engineering (Springer Science & Business Media B.V.), 2015. **18**(2): p. 115-121.

17. Sadler, Z., *Initial estimation of the in vivo material properties of the seated human buttocks and thighs.* International journal of non-linear mechanics. **107**: p. 77-85.
18. A. Duck, F., *Physical Properties Of Tissue: A Comprehensive Reference Book*. 1990.
19. Kalra A, L.A., Al-Jumaily AM, *Mechanical Behaviour of Skin: A Review*. J Material Sci Eng 2016. **5**(254).
20. G Budynas, R., *Advanced strength and applied stress analysis / Richard G. Budynas*. 2019.
21. Widdle, R.D., Bajaj, A.K., and Davies, P., *Measurement of the Poisson's ratio of flexible polyurethane foam and its influence on a uniaxial compression model.* International Journal of Engineering Science, 2008. **46**(1): p. 31-49.
22. Mills, N. and Gilchrist, A., *Modelling the indentation of low density polymer foams.* Cellular polymers, 2000. **19**(6): p. 389-412.
23. Vincent, W.J., *Statistics in Kinesiology*, ed. L.D. Robertson. 1999, California, Northridge: California State University.
24. Rahaman, M.N., *Non-linear viscoelastic properties of solid polymers.* Polymer (Guilford). **22**(5): p. 673-681.
25. Swainger, K.H., *Work-Hardening Under Complex Stresses.* Nature, 1948. **162**: p. 532.